

PREPARED FOR SUBMISSION TO JINST

DIRC WORKSHOP

11–13 SEPT 2019

CASTLE RAUISCHHOLZHAUSEN

Status of the TORCH Project

N. Harnew,^{a,1} S. Bhasin,^{b,c} T. Blake,^e N.H. Brook,^b M.F. Cicala,^f T. Conneely,^g D. Cussans,^c M.W.U. van Dijk,^d R. Forty,^d C. Frei,^d E. P. M. Gabriel,^e R. Gao,^a T. Gershon,^f T. Gys,^d T. Hadavizadeh,^a T. H. Hancock,^a M. Kreps,^f J. Milnes,^g D. Piedigrossi,^d J. Rademacker^c

^a*Denys Wilkinson Laboratory, University of Oxford, Keble Road, Oxford OX1 3RH, United Kingdom*

^b*University of Bath, Claverton Down, Bath BA2 7AY, United Kingdom*

^c*H.H. Wills Physics Laboratory, University of Bristol, Tyndall Avenue, Bristol BS8 1TL, United Kingdom*

^d*European Organisation for Nuclear Research (CERN), CH-1211 Geneva 23, Switzerland*

^e*School of Physics and Astronomy, University of Edinburgh, James Clerk Maxwell Building, Edinburgh EH9 3FD, United Kingdom*

^f*Department of Physics, University of Warwick, Coventry, CV4 7AL, United Kingdom*

^g*Photek Ltd., 26 Castleham Road, St Leonards on Sea, East Sussex, TN389 NS, United Kingdom*

E-mail: Neville.Harnew@physics.ox.ac.uk

ABSTRACT: The TORCH time-of-flight detector will provide particle identification between 2–10 GeV/c momentum over a flight distance of 10 m, and is designed for large-area coverage, up to 30 m². A 15 ps time-of-flight resolution per incident particle is anticipated by measuring the arrival times from Cherenkov photons produced in a synthetic fused silica radiator plate of 10 mm thickness. Customised Micro-Channel Plate Photomultiplier Tube (MCP-PMT) photon detectors of 53 × 53 mm² active area with a 64 × 64 granularity have been developed with industrial partners. Test-beam studies using both a small-scale TORCH demonstrator and a half-length TORCH module are presented. The desired timing resolution of 70 ps per single photon is close to being achieved.

KEYWORDS: Cherenkov detectors, Particle identification methods, Photon detectors for UV, visible and IR photons (vacuum), Timing detectors.

¹Corresponding author

Contents

1	Introduction	1
2	The photon detectors	1
3	The TORCH prototype modules and readout systems	2
4	Beam tests with the small-scale TORCH demonstrator	3
5	Beam tests with the large-scale TORCH demonstrator	4
6	Simulation of TORCH at LHCb	8
7	Conclusions and future work	8

1 Introduction

The Timing Of internally Reflected Cherenkov photons (TORCH) is a high-precision time-of-flight detector suitable for large-area applications and covering a charged-particle momentum range up to $10\text{ GeV}/c$ [1, 2]. TORCH combines timing measurements with DIRC-style reconstruction, a technique pioneered by the BaBar DIRC [3] and Belle II TOP [4] collaborations. Cherenkov photons, produced in a synthetic fused silica (quartz) radiator of 1 cm thickness, propagate by total internal reflection to focussing optics at the periphery of the detector. There the photons are detected by fast photodetectors where their arrival times and propagation angles are measured. The Cherenkov angle is then reconstructed and chromatic dispersion is accounted for in the determination of the time of propagation of each photon [2]. A schematic of the TORCH optics and modular layout is shown in Fig. 1.

At $10\text{ GeV}/c$ momentum the time of flight difference between a pion and kaon is 35 ps over a distance of 10 m, hence a time resolution of about 10-15 ps per track is required to give a 3-sigma separation. Given around 30 detected Cherenkov photons per track, a time resolution of ~ 70 ps per photon is therefore necessary. To achieve this, simulation has shown that a 1 mrad resolution of the angular measurement of each photon is required [1].

In this paper the operation of both a small- and a large-scale TORCH demonstrator module in a CERN test-beam will be described.

2 The photon detectors

The Cherenkov photons are focused onto Micro-Channel Plate Photomultiplier Tube (MCP-PMT) detectors. The MCP-PMTs have been developed in collaboration with industrial partner Photek UK in a three-phase development programme [5]. Each detector has a granularity of 64×64

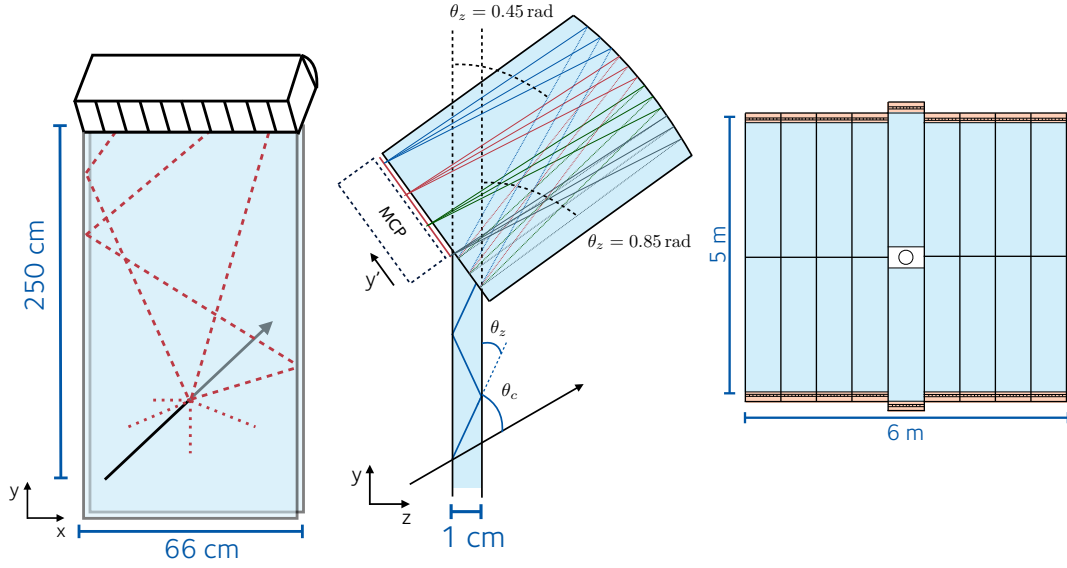


Figure 1. Schematics of the TORCH detector design. (Left) a single TORCH module, (middle) the focusing block, which translates the photon's angle of exit from the quartz plate in the yz plane (θ_z) into the y' position on the MCP-PMT detector plane, and (right) the 18-module TORCH detector proposed for LHCb.

pixels over a $53 \times 53 \text{ mm}^2$ active area. A readout PCB is connected to the pixellated anode via Anisotropic Conductive Film. Charge sharing and pixel grouping is then employed to obtain an effective granularity of 8×128 pixels, which is required to achieve the 1 mrad angular precision required by TORCH. The charge-sharing method relies on capacitive coupling to produce a smooth well-defined charge footprint on the anode [6]. This has the advantage of halving the number of anode pads in the confined area and also the number of readout channels, hence saving cost and complexity. In the coarse dimension, each of eight consecutive pixels are ganged together in the external electronics, giving eight logical pixels. By similar grouping, tubes of effective granularity 4×128 pixels have also been employed. The MCPs have ALD coating and are designed to withstand an integrated charge of 5 C/cm^2 [7, 8].

3 The TORCH prototype modules and readout systems

Two prototype modules have been tested in a number of test-beam campaigns between 2015–2018 at the CERN PS T9 beamline. The first is a small-scale TORCH demonstrator [2], and consists of a $350 \times 120 \times 10 \text{ mm}^3$ (length, width and thickness) quartz radiator plate with a matching focusing block. The demonstrator was instrumented with a single MCP-PMT, with either a 4×64 or 8×64 granularity. The second demonstrator is a prototype of a half-length TORCH module, $1250 \times 660 \times 10 \text{ mm}^3$ (length, width and thickness). This module can be instrumented with ten MCP-PMTs, although only two 8×64 MCP-PMTs were equipped for the current test-beam running, corresponding to a total of 1024 readout channels. For both demonstrators, the radiator plates were glued to the focussing blocks, supported from mounting frames, and enclosed in light-tight vessels. The radiator plates were mounted in an almost vertical position, tilted backwards by 5° with respect to the horizontal incidence of the beam.

The two types of MCP-PMTs were read out by independent fully-customised electronics readout systems [9]. The systems comprise front-end amplifier and discriminator boards, each of which houses two or four 32-channel NINO ASICs [10]. Each NINO-32 board is connected to one or two TDC boards containing a pair of HPTDC chips [11] operated in 32-channel mode, which digitise the signals with 100 ps binning. For the first small-scale demonstrator beam test with 4×64 MCP pixel readout, each NINO board had 64 channels instrumenting one column of pixels and which serviced a single HPTDC board. For the 8×64 MCP pixellization, the NINO boards were upgraded to have 128 channels instrumenting two columns of pixels and servicing a pair of HPTDC boards.

The NINO-32 provides time-over-threshold information which is used to correct time walk using a data-driven method [2]. Non-linearities of the HPTDC time digitization are also corrected. Following these offline corrections, clustering due to the charge sharing is applied over neighbouring row MCP-PMT hits, if the hits arrive within 1 ns of each other, and the centroid position of each photon hit then obtained. However the charge to width calibration has proven to be more challenging, and work is still ongoing to optimize this.

4 Beam tests with the small-scale TORCH demonstrator

The small-scale TORCH demonstrator was tested in a 5 GeV/c mixed pion/proton beam in November 2017 and June 2018. Proton-pion selection was achieved independent of TORCH using a pair of upstream Cherenkov counters. Two borosilicate finger counters (T1 and T2) separated by a ~ 11 m flight path provided a time reference. The beam was incident approximately 14 cm below the plate centre-line and close to the plate side, a position which was chosen to give a cleanly resolved pattern.

The patterns of measured photon hits are shown for both the 4×64 and 8×64 MCP-PMT configurations in Fig. 2. Hyperbola-like patterns at the MCP-PMT plane result from the Cherenkov cones which are internally reflected in the quartz radiator; reflections off the module sides result in a folding of this pattern. Chromatic dispersion spreads the lines into bands. Since only a single MCP-PMT is instrumented, the full pattern is only sampled, which accounts for the observed discontinuities. The dead channels observed in the hit distribution of the 8×64 MCP-PMT are due to NINO bonding issues (and which have since been rectified).

For each single 4-wide or 8-wide pixel column, the measured MCP time-stamp for each cluster is plotted relative to the time-stamp of the downstream borosilicate station (T2) versus the measured 64-wide row position. An example distribution for the 8×64 MCP-PMT configuration is shown in Fig. 3 (a) showing several orders of reflection, and demonstrating good agreement when compared to simulation. Figure 3 (b) highlights the corresponding photon paths. The TORCH simulation uses GEANT4 [12] to model the optical processes, including scattering, chromatic dispersion, and the response of the MCP-PMT and electronics readout. Various sources of inefficiency are included, such as the surface roughness of the quartz and the MCP-PMT quantum and collection efficiencies. An example plot of residuals between the measured times of arrival from the mean for the primary reflections and for a given MCP column is shown in Fig. 3 (c). The tails are attributed to imperfect calibrations and photoelectron backscattering from the MCP top surface. Core distributions have resolutions (sigmas) of approximately 100 - 125 ps (which is photon energy and MCP-PMT column dependent). The timing resolution of the timing reference is ~ 43 ps and, when subtracted in quadrature, gives the time resolutions presented in Table 1. These measurements are approaching

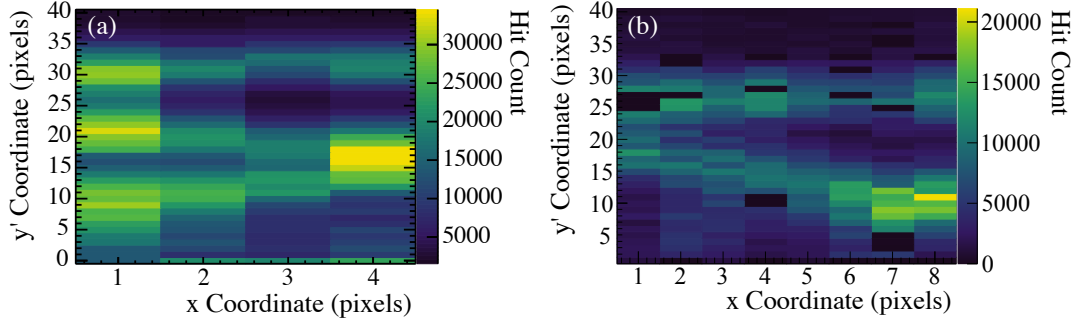


Figure 2. The patterns of hits measured in the TORCH small-scale demonstrator for a combined 5 GeV/c pion and proton beam: (a) 4×64 and (b) 8×64 pixel readout.

the target resolution of 70 ps per photon. Future improvements will be made, such as incorporating charge to width calibrations of the front-end electronics and reducing the current limitation imposed by the 100 ps time binning of the HPTDC.

MCP Column	σ_{TORCH} Pions (ps)	σ_{TORCH} Protons (ps)
1	110.6 ± 1.2	112.7 ± 1.4
2	101.7 ± 1.2	110.6 ± 1.4
3	101.5 ± 1.2	110.6 ± 1.4
4	105.5 ± 1.2	106.2 ± 1.4
5	83.8 ± 1.3	91.0 ± 1.4
6	101.3 ± 1.2	103.4 ± 1.2
7	90.3 ± 1.2	87.5 ± 1.4
8	112.4 ± 1.1	102.8 ± 1.4

Table 1. The single-photon time resolutions measured for the 8×64 MCP-PMT of the small-scale demonstrator. The MCP column numbers match those shown in Fig. 2(b). The quoted errors are purely statistical.

5 Beam tests with the large-scale TORCH demonstrator

The half-length TORCH module was tested in a 8 GeV/c mixed pion-proton beam in October 2018 [13]. The beam infrastructure was as described in Sec. 4. Two MCP-PMTs were instrumented and the spatial distribution of measured hits is shown in Fig. 4(a). The left MCP-PMT (labelled MCP-A) has a quantum efficiency which peaks at only $\sim 13\%$ and has a number of dead pixels due to disconnected NINO wire bonds. Hence, the analysis for the study presented below was based only on the right MCP-PMT (labelled MCP-B), which has a quantum efficiency peaking at $\sim 18\%$.

An example time-projection plot for a single column of MCP-B as a function of pixel hit is shown in Fig. 4(b), along with the predictions from the reconstruction. It can be seen that several

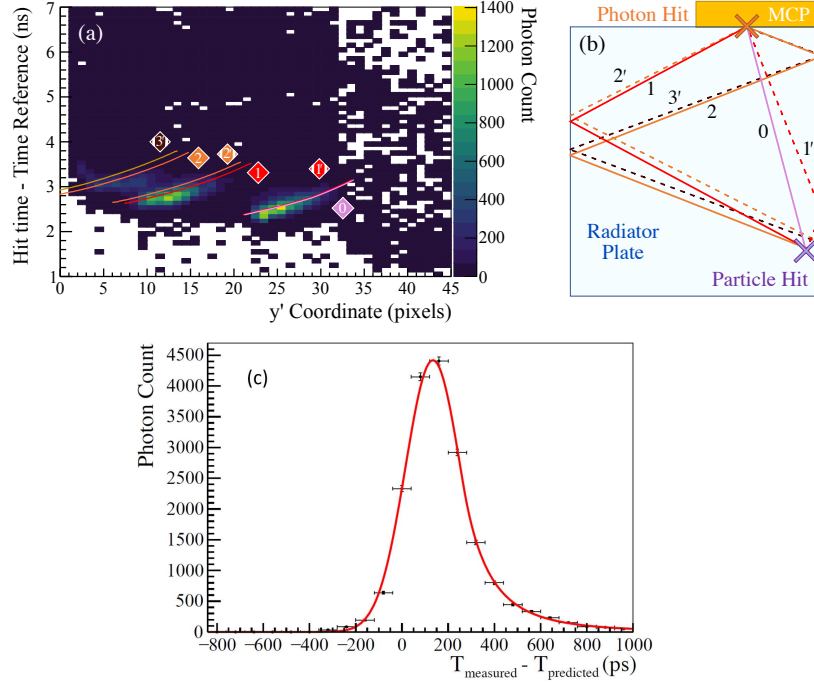


Figure 3. (a) The time-of-arrival of single Cherenkov photons in the small-scale TORCH demonstrator for 5 GeV/c pions, relative to the T2 beam time-reference station, as a function of detected 64-wide row pixel number for column 5 of the 8×64 MCP-PMT configuration. The overlaid lines represent the simulated patterns. (b) A schematic of the photon paths assigned in the reconstruction which correspond to the overlaid lines in (a), labelled according to the number of side reflections the photon undergoes. Paths first reflecting off the edge closest to the beam are shown by dashed lines, and their label has a prime. (c) An example plot of residuals between the measured times of arrival from the predicted mean distribution for the 0 and 1' reflections.

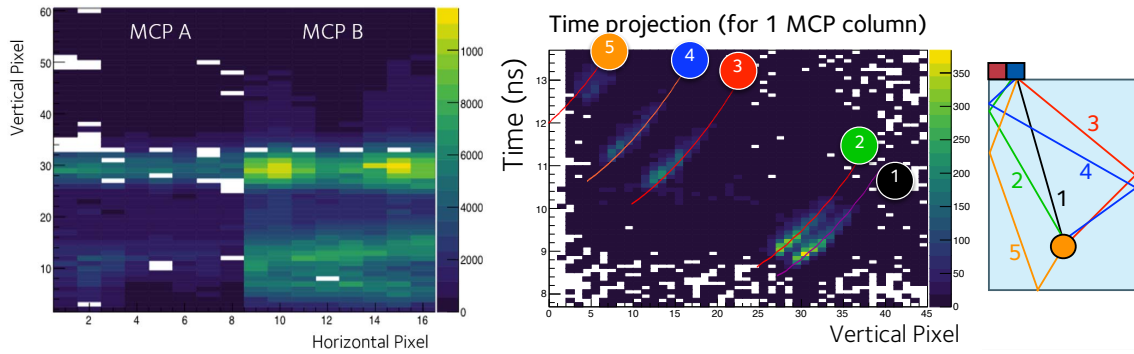


Figure 4. (Left) The spatial distribution of hits on the two MCP-PMTs of the half-length TORCH module, labelled MCP-A and MCP-B. 16 channels were read out for the time reference, indicated by the central white band of empty hits (vertical pixel row 32). (Middle) The time projection of a single MCP-PMT column versus hit pixel number, with the photon trajectories labelled as shown in the diagram on the right.

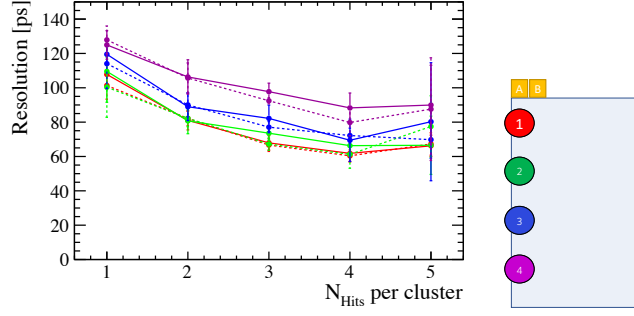


Figure 5. The single-photon time resolution for the half-length TORCH module as a function of the number of hits per cluster, as determined for the beam positions colour-coded in the diagram on the right. The solid lines are for pions, the dotted lines for protons. The vertical positions from the MCP-PMT plane are 17.5 cm (top), 45.3 cm, 73.2 cm and 101.0 cm (bottom).

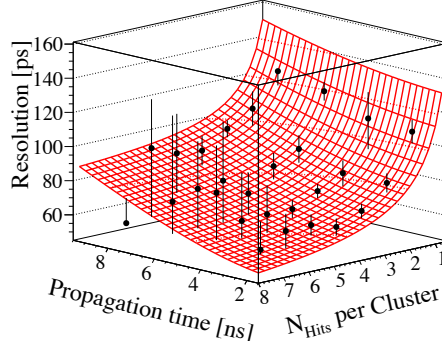


Figure 6. The TORCH time resolution as a function of the photon propagation time and number of hits per cluster. The overlaid surface is the result of a 2D fit, described in the text.

orders of side reflection are cleanly separated. As for the small-scale demonstrator, the widths of each order are measured from fits to determine the single-photon time resolution for that MCP column. The time resolution is then corrected for the uncertainty arising from the time reference pulse (~ 43 ps) and from the beam spread uncertainty ($\sim 15 - 30$ ps, which is dependent on the distance between the beam entry point and the MCP-PMT plane).

The vertical distance of the beam incidence position in the quartz to the MCP-PMT plane was varied from 17.5 cm to 101.0 cm in four steps. The measured time resolutions for first-order reflections are shown in Fig. 5 as a function of the number of hits per cluster, corresponding to all photon clusters that contain between 2 and 5 hits. Some degradation of the time resolution with distance of photon propagation is observed, however this reduces as the size of the cluster increases. The single-photon time resolution approaches or matches the design goal of 70 ps for specific beam positions and cluster sizes.

The contributions to the timing resolution, σ_{TORCH} , can be attributed to the sources defined in the following expression:

$$\sigma_{\text{TORCH}}^2 = \sigma_{\text{const}}^2 + \sigma_{\text{prop}}^2(t_P) + \sigma_{\text{RO}}^2(N_{\text{Hits}}). \quad (5.1)$$

Here the constant contribution, σ_{const} , includes sources such as the intrinsic MCP-PMT time reso-

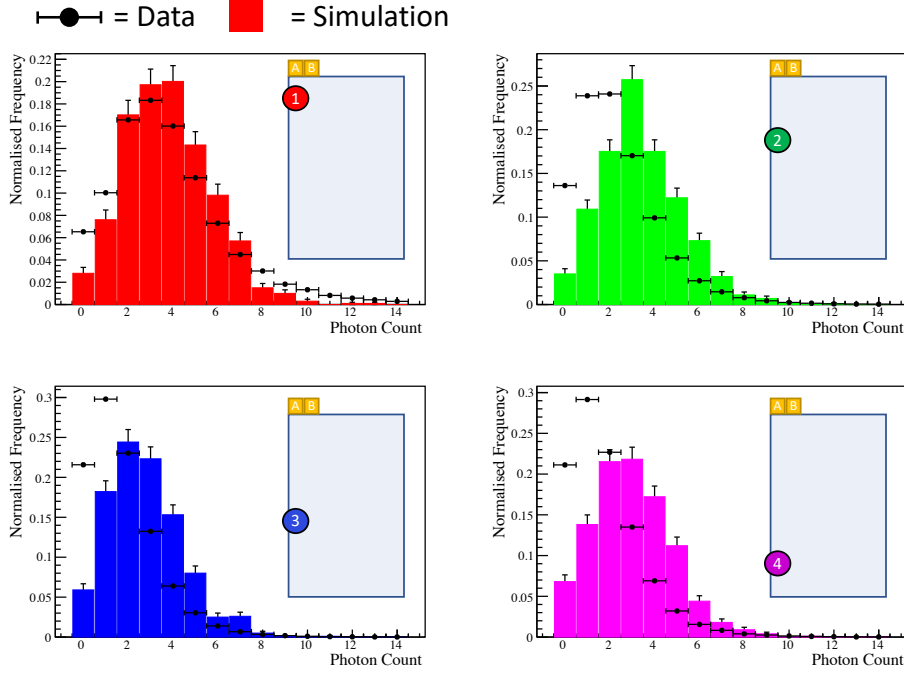


Figure 7. Photon yields in data (points) and simulation (histograms) when the beam is positioned 17.5 cm (top left), 45.3 cm (top right), 73.2 cm (bottom left) and 101.0 cm (bottom right) from the MCP-PMT plane.

lution, the term $\sigma_{\text{prop}}(t_P)$ characterises the contributions that grow linearly with photon propagation time, t_P , such as dispersive effects, and finally the term $\sigma_{\text{RO}}(N_{\text{Hits}})$ which is inversely proportional to the square root of the number of hits in a cluster, N_{Hits} . A two dimensional fit, shown in Fig. 6, has been performed to the time resolution as a function of t_P and N_{Hits} , with best-fit values as follows:

$$\sigma_{\text{const}} = 33.0 \pm 7.1 \text{ ps},$$

$$\sigma_{\text{prop}}(t_P) = (7.8 \pm 0.7) \times 10^{-3} \times t_P [\text{in ps}], \text{ and}$$

$$\sigma_{\text{RO}}(N_{\text{Hits}}) = \frac{100.5 \pm 5.7}{\sqrt{N_{\text{Hits}}}} \text{ ps}.$$

Further studies of these contributions are currently underway, and improvements can be expected with refined electronics calibrations in the future.

The number of photon clusters measured in the half-length demonstrator are compared to simulation in Fig. 7. Reasonable agreement is seen when the beam is close to the MCP-PMTs, but discrepancies are observed when the photon path becomes longer, an effect which is currently under study. As the half-length prototype is instrumented with only two MCP-PMTs out of the design total of eleven, the light yield is expected to improve by a factor of 5.5 in the fully instrumented module. Additionally, the peak quantum efficiencies of the final MCP-PMTs are expected to have a factor ~ 2 improvement, further increasing the photon yield to meet the 30 targeted.

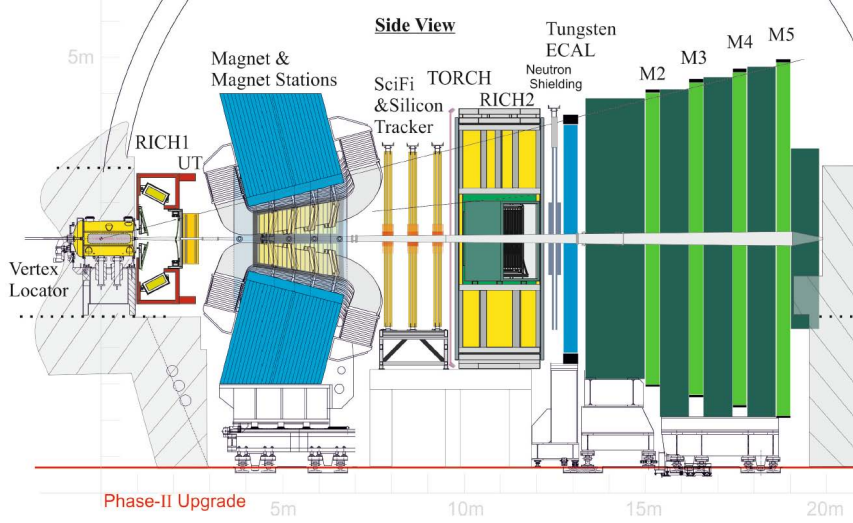


Figure 8. A schematic of the LHCb experiment, showing TORCH located directly upstream of the RICH 2 detector.

6 Simulation of TORCH at LHCb

An exciting application of TORCH is for the LHCb Upgrade II experiment, where the detector would occupy an area of $5 \times 6 \text{ m}^2$ in front of the current RICH 2 detector to complement the experiment's particle identification (PID) capabilities, covering up to $10 \text{ GeV}/c$ and beyond [14, 15]. The full TORCH detector would comprise 18 modules with 198 MCP-PMTs, and studies are ongoing to simulate the TORCH performance in GEANT4. The proposed experimental location together with the modular arrangement are shown in Figs. 8 and 1, respectively.

The TORCH PID performance has been determined for the LHCb Upgrade (Run 4) conditions at an instantaneous luminosity of $\mathcal{L} = 2 \times 10^{33} \text{ cm}^{-2} \text{ s}^{-1}$. Figure 9 shows the efficiency for TORCH to positively identify kaons as a function of momentum and the probability that pions are misidentified as kaons. This demonstrates that the TORCH detector has excellent separation power in the range up to $10 \text{ GeV}/c$ for kaons and pions, and up to $20 \text{ GeV}/c$ for kaons and protons. This work will form the basis of a Technical Proposal to construct a full-scale TORCH detector for the start-up of LHC Run 4, for installation in the Long Shutdown 3 (LS3).

7 Conclusions and future work

TORCH is an innovative detector concept designed to achieve a time-of-flight resolution of 15 ps, providing a $\pi - K$ separation up to $10 \text{ GeV}/c$ momentum over a 10 m flight path. A successful series of beam tests has been conducted with both a small-scale TORCH demonstrator and a half-length module. Customised MCP-PMTs have been employed which satisfy the TORCH requirements of lifetime, granularity and active area. Single-photon time resolutions have been measured in the range 60–130 ps, achieving the goal of 70 ps in some configurations. Further laboratory tests are ongoing to independently verify the contributions to the time resolution, and improved electronics calibrations are expected to further enhance the performance.

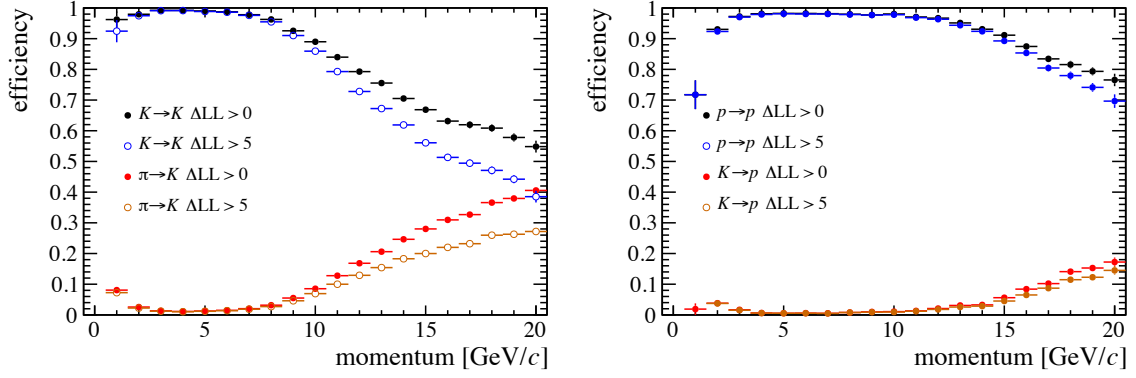


Figure 9. The efficiency in LHCb for TORCH (left) to positively identify kaons as a function of momentum and the probability that pions are misidentified as kaons and (right) the same plots for kaons and protons. The curves are for two different delta-log-likelihood cuts and for a luminosity of $2 \times 10^{33} \text{ cm}^{-2}\text{s}^{-1}$.

A full-scale 18-module TORCH detector has been simulated in the LHCb experiment and these studies indicate that significant improvements in the experiment’s particle identification capabilities can be expected. The half-length TORCH module will be instrumented with 10 MCP-PMTs, and will be tested in the future months.

Acknowledgments

The support of the European Research Council through an Advanced Grant under the Seventh Framework Programme (FP7), ERC-2011-AdG 299175-TORCH, and the Science and Technology Research Council, UK, through grant number ST/P002692/ are acknowledged. The Corresponding Author (NH) would like to thank the organisers of DIRC2019 for their support, and for hosting such an enjoyable Workshop.

References

- [1] M. Charles and R. Forty, *TORCH: Time of flight identification with Cherenkov radiation*, *Nucl. Instrum. Meth.* **A639** (2011) 173.
- [2] N. H. Brook *et al.*, *Testbeam studies of a TORCH prototype detector*, *Nucl. Instrum. Meth.* **A908** (2018) 256.
- [3] I. Adam *et al.*, *The DIRC Particle Identification System for the BABAR Experiment*, *Nucl. Instrum. Meth.* **A538** (2005) 281.
- [4] J. Fast (Belle-II Particle Identification Group), *The Belle II imaging Time-of-Propagation (iTOP) detector*, *Nucl. Instrum Meth.* **A876** (2017) 145.
- [5] N. Harnew *et al.*, *Status of the TORCH time-of-flight project*, *Nucl. Instrum. Meth.* **A952** (2020) 161692.
- [6] T. M. Conneely, J. Lapington, J. S. Milnes (Photek Ltd), *Simulation studies of a novel, charge sharing, multi-anode MCP detector*, *PoS(TIPP2014)* 306.

- [7] T. M. Conneely, J. S. Milnes, J. Howorth (Photek Ltd), *Characterisation and lifetime measurements of ALD coated microchannel plates in a sealed photomultiplier tube*, *Nucl. Instrum. Meth.* **A732** (2013) 388.
- [8] T. Gys *et al.*, *Performance and lifetime of micro-channel plate tubes for the TORCH detector*, *Nucl. Instrum. Meth.* **A766** (2014) 171.
- [9] R. Gao *et al.*, *Development of TORCH readout electronics for customised MCPs*, *JINST* **11** C04012 (2016).
- [10] F. Anghinolfi *et al.*, *NINO: an ultra-fast and low-power front-end amplifier/discriminator ASIC designed for the multigap resistive plate chamber*, *Nucl. Instr. and Meth.* **A533** (2004) 183.
- [11] J. Christiansen, *High Performance Time to Digital Converter*, CERN/EP-MIC, 2002.
- [12] J. Allison *et al.*, *Recent developments in GEANT4*, *Nucl. Instrum. Meth.* **A835** (2016) 186.
- [13] T. H Hancock, *et al.*, *Beam tests of a large-scale TORCH time-of-flight demonstrator*, *Nucl. Instr. and Meth.* **A958** (2020) 162060.
- [14] I. Bediaga *et al.*, *LHCb particle identification upgrade*, LHCb TDR 14, CERN-LHCC-2013-022.
- [15] R. Aaij *et al.*, *Physics case for an LHCb Upgrade II - Opportunities in flavour physics, and beyond, in the HL-LHC era*, LHCb-PUB-2018-009, CERN-LHCC-2018-027.